Polytechnic Journal

Polytechnic Journal

Volume 14 | Issue 1 Article 12

Cantor Set from a Nonstandard Viewpoint

Sebar H. Jumha

Department of Mathematics, College of Science, Salahaddin University-Erbil, Erbil (Hawler), Kurdistan Region, Iraq

Ibrahim O. Hamad

Department of Mathematics, College of Science, Salahaddin University-Erbil, Erbil (Hawler), Kurdistan Region, Iraq, ibrahim.hamad@su.edu.krd

Ala O. Hassan

Department of Mathematics, College of Science, Salahaddin University-Erbil, Erbil (Hawler), Kurdistan Region, Iraq

How to Cite This Article

Jumha, Sebar H.; Hamad, Ibrahim O.; and Hassan, Ala O. (2024) "Cantor Set from a Nonstandard Viewpoint," *Polytechnic Journal*: Vol. 14: Iss. 1, Article 12.
DOI: https://doi.org/10.59341/2707-7799.1830

Cantor Set from a Nonstandard Viewpoint

Data Availability Statement

The data supporting the findings of this study are publicly available and are included within this published article.

AI Usage Declaration

The authors declare that the content of this work was not generated using AI.

Acknowledgments

The authors sincerely acknowledge the support and contributions of their university and all individuals who assisted in the completion of this study.

ORIGINAL ARTICLE

Cantor Set From a Nonstandard Viewpoint

Sebar Haji Jumha, Ibrahim Othman Hamad*, Ala Omer Hassan

Department of Mathematics, College of Science, Salahaddin University-Erbil, Erbil (Hawler), Kurdistan Region, Iraq

Abstract

This paper proposes a fresh perspective for visualizing the Cantor set and explores its shading characteristics through the utilization of nonstandard tools and techniques. Our investigation reveals that the measure of the Cantor set is infinitely close to zero but not identically zero, and we validate the properties of the Cantor set using an assortment of nonstandard methodologies. These findings have far-reaching implications for enhancing our understanding of mathematical approximations and exact measurements. Furthermore, we correlate our nonstandard perspective outcomes regarding the Cantor set with some specific applied models.

MSC: 26E35, 03H05, 97F70, 28E05

Keywords: Nonstandard, Cantor set, Infinitely close, Measure zero, Uncountable set

1. Introduction

Nonstandard Analysis (NSA) constitutes a mathematical framework that supplements conventional mathematical principles through the incorporation of alternative tools and methodologies. It serves as a facilitator for the substantiation of classical theorems and findings. Simultaneously, empirical research has demonstrated that nonstandard concepts, while proven equivalent to their standard counterparts, retain an inherent distinctiveness. Abraham Robinson's development in analysis revolutionized the field by introducing infinitesimals and unlimited quantities, there by resolving the longstanding issue of the infinitely small in Leibniz's definition of definite integral [1,2].

Robinson's achievement is a significant milestone in the history of mathematics. Leibniz employed the concept of infinitesimals indirectly in the formulation of the derivative and integral. The incorporation of nonstandard methodologies in contemporary mathematics has expanded the horizons for researchers engaged in the exploration of innovative mathematical domains. For more examples of this see Tiwari and Giordano [3], Golbaltt [4], Qadir and et al. [5], Hamad and Ismail [6], … etc.

The conventional formula for calculating the measure of the interval $I=(a,b)$ denoted by $m(I)$, is defined as follows:

$$m(I)=\begin{cases} b-a & \text{if } I=(a,b) \\ 0 & \text{if } I=\varnothing \end{cases}$$

This paper relies on the use of various definitions and theorems, which are essential for the proper understanding of the presented results. Below are some of these definitions and theorems:

Definition 1.1. [7]
An element $x\in\mathbb{R}^*$ is

- Infinitesimal if $|x|<r$ for all positive real r,
- Limited if $|x|<r$ for some real r,
- Unlimited if $|x|>r$ for all real r.

Lemma 1.2. [8]
In the hyperreal number system $\mathbb{R}^*$, the following properties holds:
Let γ and δ be infinitesimals, x and y be limited, α and β be unlimited (all in $\mathbb{R}^*$). Then

1. $\gamma+\delta, \gamma\delta, \gamma x$, and α^{-1} are infinitesimals.
2. $\delta+x, x+y, xy$, and $x^{-1}(x\neq 0)$ are limited.

Received 24 May 2024; accepted 30 June 2024.
Available online 30 July 2024

* Corresponding author.
E-mail addresses: sebar.jumha@su.edu.krd (S.H. Jumha), ibrahim.hamad@su.edu.krd (I.O. Hamad), ala.hassan@su.edu.krd (A.O. Hassan).

https://doi.org/10.59341/2707-7799.1830

3. $\alpha+\beta, \alpha\beta$, and $\delta^{-1}(\delta\neq 0)$ are unlimited.
4. Every infinitesimal is limited.
5. Zero is the only standard infinitesimal.

Definition 1.3. [9]
For $x, y\in\mathbb{R}^*$, we say x and y are infinitely close, denoted by $x\simeq y$, if $x-y$ is infinitesimal.

Definition 1.4. [7]
Given a number $x\in\mathbb{R}^*$, then monad $(x) = \{y\in\mathbb{R}^* : y\simeq x\}$.

Theorem 1.5. (Existence of Standard Parts) [9]
If r is limited hyperreal number, then there exists a unique $s\in\mathbb{R}^*$ such that $r\simeq s$. The number s is called the standard part or (shadow) of r and denoted by $st(r)$ or ${}^o r$.

Definition 1.6. [1]
A collection of mathematical rules or expressions that do not involve any new concepts or assumptions such as (standard, infinitesimal, limited, unlimited, … etc.) are referred to as internal. Otherwise, they are classified as external.
In 1977, Eduard Nelson [1] proposed a new structure for the NSA based on the following three principles:
Transfer Principle (T) Let A be an internal formula with the only free variables are $x, t_1, t_2, \ldots, t_n$. Then

$$\forall^{st} t_1 \ldots \forall^{st} t_n [\forall^{st} x A \Leftrightarrow \forall x A].$$

The Idealization Principle (I) Let A be an internal formula. Then

$$\forall^{stfin} x' \exists y \forall x\in x' A \Leftrightarrow \exists y \forall^{st} x A.$$

The Standardization Principle (S) Let F be an internal or external formula with free variables z and optionally additional variables. Then $\forall^{st} X \exists^{st} Y \forall^{st} z [z\in Y \Leftrightarrow z\in X \wedge F(z)]$,
where the symbols; *st*, *stfin* are denotes to the terms standard and standard finite respectively.
The Standardization Principle enables the definition of standard subsets using standard elements. In other words, it states that there exists a standard set Y, such that a standard element z belongs to Y if and only if it belongs to in X and $F(z)$ holds. In the context of nonstandard hyperreal numbers, open and closed sets can be defined as follows:

Definition 1.7. [10]
Let (X, d) be a metric space and E be a subset of X. Assume that $x\simeq y$ if and only if $d(x, y)\simeq 0$. Then

i. x^{st} is limit point in E if $y\in E$ for some $y\simeq x$ and $y\neq x$.
ii. x is nearly standard if $\exists^{st} y, x\simeq y, y = \widehat{A}^{\circ} x$.
iii. E^{st} is compact if $\forall x\in E \Rightarrow \exists^{st} x_o \in E, x\simeq x_o$.
iv. E^{st} is open if $\forall^{st} x\in E$ and $\forall x_o, x_o\simeq x \Rightarrow x_o\in E$.
v. E^{st} is closed if $\forall x\in E$ and $\forall^{\mathrm{st}} x_o, x_o\simeq x \Rightarrow x_o\in E$.

Definition 1.8. [8]
Let A^* be a subset of $\mathbb{R}^*$. Then $x\in A^*$ is said to be a closure point of A^* if and only if monad $(x)\cap A^*\neq\varnothing$.

Definition 1.9. [8]
Let A^* be a subset of $\mathbb{R}^*$. Then $x\in A^*$ is said to be an isolated point of A^* if and only if monad $(x)\cap A^*\neq\varnothing$, while monad $(x)\cap A^*\setminus\{x\} = \varnothing$.

Theorem 1.10. [11]
Every countable set has a measure of zero.

Definition 1.11. [12]
Given a set $A\subset\mathbb{R}$, we say that A is nowhere dense, if every open interval I contains an open subinterval $J\subset I$, such that $J\cap A = \varnothing$. Alternatively, if int $(\overline{A}) = \varnothing$, where int $(\overline{A})$ is denoted to the interior of the closure of the set A.

Theorem 1.12. [13]
If A is a closed and bounded subset of real numbers, then A is compact.

Definition 1.13. [13]
A set $A\subset\mathbb{R}$ is perfect if and only if it is closed and does not contain any isolated points.

Lemma 1.14. (Robinson's Lemma) [4,14]
If $\{a_n\}_{n\in\mathbb{N}}$ is an internal sequence of real numbers such that $a_n\simeq 0$ for all $n\in\mathbb{N}$ then there exists unlimited $\omega\in\mathbb{N}^*$ such that $a_n\simeq 0$ for all $n\leq\omega$.

Theorem 1.15. (Robinson's characterization of compactness) [2]
K is compact if for all $p\in K^*$ there is $q\in K$ with $p\simeq q$.

Definition 1.16. [15]
A nonempty set $C^*\subset\mathbb{R}^*$ is Cantor set if and only if C^* is perfect and nowhere dense.

2. Nonstandard structure of cantor set and its properties

Let U be an open set in the hyperreal number space $\mathbb{R}^*$ introduced by finite or infinite sequence of disjoint open intervals $\{J_n\}$ consisting of rational numbers, that is $U = \bigcup_{n=0}^{\infty}\{J_n\}$, and if necessary, assume that $J_n = \varnothing$ for sufficiently large (unlimited) n. We denote the measure of an interval J, if it exists, by $m(J)$. Consequently, the measure of an interval U can be defined as $m(U) = \sum_{n=0}^{\infty} m(J_n)$, provided that the sum on the right-hand side is exists. It is possible to utilize Transfer Principle to define the measure of $m(U)$ in $\mathbb{R}^*$. By allowing ε to be infinitesimal and k to

be a unlimited positive integer, we can express U as the sum of U_1 and U_2, where $U_1 = \bigcup_{n=0}^{k} J_n$ is the union of a finite sequence of open intervals, and the measure of $U_2 = \bigcup_{n=k+1}^{\infty} J_n$ is infinitesimal, which is equivalent to $m(U_2) \simeq 0$. Traditionally, the Cantor set is defined as a subset of the closed interval $[0, 1]$. However, in a broader context, the Cantor set can be defined as a subspace of $\mathbb{R}$ with remarkable topological characteristics. Specifically, the Cantor set is a totally disconnected, compact, metrizable, and uncountable space. The construction of the Cantor set involves iteratively removing the open middle third from a closed interval, followed by removing the open middle third of the two remaining intervals, and so on. Geometrically, the Cantor set can be visualized as the result of continuously removing parts from a set.

This paper aims to present an alternative nonstandard approach for defining and understanding the properties of the Cantor set. The traditional approach of the variety method is limited in its ability to fully describe the Cantor set. By utilizing nonstandard analysis, we can provide a more comprehensive and precise representation of the Cantor set and some of its characteristics. Let $[0,1]^*$ be a unit closed subset of $\mathbb{R}^*$ represent the nonstandard extend of the classical unit closed interval $[0, 1] \subseteq \mathbb{R}$. Let $C_o^* = [0,1]^*$ and define $C_1^* = \left[0,\frac{1}{3}\right]^* \cup \left[\frac{2}{3},1\right]^*$. Then $C_1^* = C_o^* \setminus \left(\frac{1}{3},\frac{2}{3}\right)^*$. Next C_2^* is derived from C_1^* by removing the open middle thirds from $\left[0,\frac{1}{3}\right]^*$ and $\left[\frac{2}{3},1\right]^*$ to get $C_2^* = \left[0,\frac{1}{9}\right]^* \cup \left[\frac{2}{9},\frac{1}{3}\right]^* \cup \left[\frac{2}{3},\frac{7}{9}\right]^* \cup \left[\frac{8}{9},1\right]^*$. In general by the results given by Pawłowiczin in [16], we obtain that for all $i \in \mathbb{N}^*$, $C_i^* = \bigcup_{n=1}^{2^i} [l_i^n, r_i^n]^*$, where $l_i^{(n)} = \frac{a_i^{(n)}}{3^i}, r_i^{(n)} = \frac{a_i^{(n)}+1}{3^i}$, and $a_i^{(n)}$ are given by the recursive formula $a_o^{(1)} = 0, \ldots, a_{i+1}^{(n)} = a_i^{(n)}, \ldots, a_{i+1}^{(2^i+n)} = a_i^{(n)} + 2 \times 3^i, n = 1, 2, \ldots, 2^i$, and C_i^* is the union of 2^i pairwise disjoint closed sets for all $i \in \mathbb{N}^*$. It's obvious that $C_o^* \supset C_1^* \supset C_2^* \supset \cdots$. We define the nonstandard Cantor set to be $C^* = \bigcap_i C_i^*$, $i \in \mathbb{N}^*$, with the measure of every disjoint closed set equal to $\frac{1}{3^i}$ for all $i \in \mathbb{N}^*$. The general form of nonstandard Cantor set sub intervals at unlimited iterative index ω will be equal to the collection $\left\{\left[0,\frac{1}{3^\omega}\right]^*, \ldots, \left[1-\frac{1}{3^\omega},1\right]^*\right\}$, with each interval having an infinitesimal measure. Therefore, $C_\omega^* = \left[0,\frac{1}{3^\omega}\right]^* \cup , \ldots, \bigcup \left[1-\frac{1}{3^\omega},1\right]^*$.

The classical definition of the Cantor set is $C = \bigcap_{i=1}^{\infty} C_i$. Robinson's lemma 1.14 assert that there exists an unlimited $\omega \in \mathbb{N}^*$ such that $C^* = \bigcap_{i=1}^{\omega} C_i{}^*$. The following are some nonstandard treatments of Cantor set.

Theorem 2.1. Cantor set is nonempty set.

Proof: Let C_i^*, for all $i \in \mathbb{N}^*$ be the closed sets previously defined. Given that $C^* = \bigcap_{i=1}^{\omega} C_i^*$, then C^* contains all the boundary points of infinite union closed sets. For instance, when $C_0{}^* = [0,1]^*$ and $C_1^* = \left[0,\frac{1}{3}\right]^* \cup \left[\frac{2}{3},1\right]^*$, we observe that $0, \frac{1}{3}, \frac{2}{3}, 1$ belong to both sets. Moreover, $C_o^* \supset C_o^* \supset C_2^* \supset \cdots$ Additionally, $C_i{}^*$ is the union of 2^i pairwise disjoint closed sets for all $i \in \mathbb{N}^*$, and we see that $C_i^* = \bigcup_{n=1}^{2^i} [l_i^n, r_i^n]^*$ for all $i \in \mathbb{N}^*$, which contains all the boundary points of C_i^*. Hence, C^* is not empty set.

Theorem 2.2. Cantor set is closed set.

Proof: The set C_ω^* is obtained by removing ω open intervals from $C_{\omega-1}^*$. Since $C^* = \bigcap_i^{\omega} C_i^*$, for unlimited index $\omega \in \mathbb{N}^*$, then to prove that C^* is the closed set, we start with the set $C_o^* = [0,1]^*$. Now for all $x \in [0,1]^*$ and any standard x_o such that $x_o \simeq x$, we have $x_o \in [0,1]^*$. Thus, C_o^* is closed in $\mathbb{R}^*$. Similarly, we can prove that the intervals $\left[0,\frac{1}{3}\right], \left[\frac{2}{3},1\right], \cdots, \left[1-\frac{1}{3^i},1\right]^*$ are closed. It follows that for all $i \in \mathbb{N}^*$, $C_i{}^* = \bigcup_{n=1}^{2^i} [l_i^n, r_i^n]^*$ is closed. Therefore, $C^* = \bigcap_i C_i^*$ is closed.

Nonstandard analysis provides a significant advantage in studying the Cantor set by enabling an accurate determination of the set's actual measure. The measure of the Cantor set is an infinitesimal quantity that is not identically zero. The following theorem illustrates this fact.

Theorem 2.3. The measure of Cantor set C^* in $\mathbb{R}^*$ is infinitesimal. That is $m(C^*) \neq 0$.

Proof: Given that C_i^* is a union of 2^i pairwise disjoint closed sets for all $i \in \mathbb{N}^*$ with a measure of each disjoint closed set being $\frac{1}{3^i}$, it follows that C_ω^* can be seen as a set with infinitesimal distance. Therefore, $m(C^*) = \sum_{i \in \mathbb{N}^*} m(C_i^*)$. By reversing the index arrangement of each C_i^* up to an unlimited index ω, we obtain ω-subintervals of measure $\frac{1}{3^{\omega+1}}$, without loss of generality, we have $m(C_i^*) \simeq m(C_{i+1}^*)$ for $i = \omega, \omega + i, \omega + 2, \ldots$.

This result indicates that $m(C^*) \simeq \sum_{i=\omega}^{\infty} m(C_i^*) \simeq \omega \frac{1}{3^\omega}$. But

$$\omega \frac{1}{3^\omega} = \omega \left(\frac{1}{3}\right)^\omega = \omega e^{\omega \ln\left(\frac{1}{3}\right)} = \omega e^{-\omega \ln(3)} = \omega e^{-\omega t} = \frac{\omega}{e^{\omega t}}$$

where $t = \ln(3)$. Mention that the Taylor series for $e^{\omega t}$ is

$$e^{\omega t} \simeq \left[1+\omega t+\frac{(\omega t)^2}{2!}+\ldots+\frac{(\omega t)^i}{i!}\right]$$
$$\simeq \omega\left[\frac{1}{\omega}+t+\frac{\omega t^2}{2!}+\ldots+\frac{\omega^{i-1}t^i}{i!}\right]$$

Since ω is unlimited, then by Lemma 1.2 (1), we have $\frac{1}{\omega}$ is infinitesimal.
Therefore, $e^{\omega t} \simeq \omega\left[t+\frac{\omega t^2}{2!}+\ldots+\frac{\omega^{i-1}t^i}{i!}\right]$.
Since $t = \ln(3)$ is appreciable, then $\left[t+\frac{\omega t^2}{2!}+\ldots+\frac{\omega^{i-1}t^i}{i!}\right]$ is become an unlimited quantity greater than ω, represented it by ω^*, hence $e^{\omega t} \simeq \omega \cdot \omega^*$. Consequently, $\frac{\omega}{e^{\omega t}} \simeq \frac{\omega}{\omega(\omega^*)} = \frac{1}{\omega^*}$, which is an infinitesimal.
Therefore, $m(C^*) = \sum_{i=\omega}^{\infty} m(C_i^*) \simeq \frac{\omega}{e^{\omega t}} \simeq \frac{\omega}{\omega(\omega^*)} = \frac{1}{\omega^*} \simeq 0$. In conclusion, the measure of the Cantor set C^* is infinitesimal not identically zero. Thus $m(C^*) \neq 0$.

Corollary 2.4. Cantor set is uncountable set.

Proof: By Theorem 2.3 the measure of the Cantor set C^* in nonstandard sense is infinitesimal not identically zero and then by Theorem 1.10, we conclude that the Cantor set is uncountable.

Theorem 2.5. Cantor set has no isolated points.

Proof: We need to prove that every element in the Cantor set is a closure point. This means we have to show that for any $x \in C^*$, monad $(x) \cap C^* \setminus \{x\}$ is non empty set. It is clear that monad $(x) \cap C^* \neq \emptyset$ for all $x \in C^*$. Using Definition 1.7 (ii) and take $x, y \in C^*$ such that $x = 0$ and $y = \frac{1}{3^\omega} \in C^*$ where ω is an unlimited natural number. Therefore, $\frac{1}{3^\omega} \in \left[0, \frac{1}{3^{\omega-1}}\right]^* \subset C^*$. Subsequently, monad (0) $\bigcap \left[0, \frac{1}{3^{\omega-1}}\right]^* \neq \emptyset$. Hence, monad $(0) \cap C^* \neq \emptyset$. This assumption is repeated for each $x \in C^*$ in order to arrive at the conclusion that monad $(x) \cap C^* \neq \emptyset$. Hence, x is not an isolated point in C^*.

Theorem 2.6. Cantor set is nowhere dense.

Proof: According to Theorem 2.2, the Cantor set is closed set. Therefore, $\overline{C^*} = C^*$, and by Theorem 2.3, we have $m(C^*) \simeq 0$, then we conclude that $m(\overline{C^*}) = m(C^*) \simeq 0$. Hence, $m(\overline{C^*}) \simeq 0$, indicating that $\overline{C^*}$ cannot contain a standard open interval. Therefore, int $(\overline{C^*}) = \emptyset$. Hence, C^* is nowhere dense in $[0,1]^*$.

Theorem 2.7. Cantor set is a perfect set.

Proof: Using Theorems 2.2 and 2.5, we can conclude that the Cantor set is a closed set without any isolated points. Therefore, according to Definition 1.13, the Cantor set is a perfect set.

Theorem 2.8. The standardization of the Cantor set is closed set.

Proof: According to the Standardization Principle (S), it is essential to demonstrate that $(C^*)^{st} = \bigcap_{i=0}^{\infty} (C_i^*)^{st}$, for all $i \in \mathbb{N}^*$. Let $C_o^* = [0,1]^*$. Then, by Definition 1.7 (v), if $x \in [0,1]^*$ and a standard x_o such that $x_o \simeq x$, then $x_o \in [0,1]^*$. Since $(C_0^*)^{st}$ is closed, we conclude that $(C_1^*)^{st}$ is also closed. Assuming that $C_1^* = \left[0, \frac{1}{3}\right]^* \cup \left[\frac{2}{3}, 1\right]^*$ is closed, it follows that for any $x \in C_1^*$ and any standard x_o, if $x_o \simeq x$, then $x_o \in C_1{}^*$. By repeating this procedure up to the ω-step, we find that $(C_\omega^*)^{st} = \bigcup_{i=0}^{\omega} (T_i^*)^{st}$, where all T_i^* are closed in $\mathbb{R}^*$ for all $i \in \mathbb{N}^*$. Thus $(C_\omega^*)^{st}$ is closed. Consequently, $(C^*)^{st} = \bigcap_{i=0}^{\infty} (C_i^*)^{st}, i \in \mathbb{N}^*$, is closed.

Lemma 2.9. Cantor set is compact set.

Proof: Nonstandard Cantor set C^* is bounded due to the fact that $C^* \subset [0,1]^*$ and is closed by Theorem 2.2, so it is compact by the Transfer Principle (T) and Theorem 1.12.

Theorem 2.10. The standardization of Cantor set is compact.

Proof: The Cantor set C is a standard and compact. According to Theorem 1.15, for any $x \in C^*$, there exists $x_o \in C$ such that $x_o \simeq x$. The task now is to show that whether $x_o \in C^*$. Theorem 2.8 proves that $(C^*)^{st}$ is closed, and by Definition 1.7 (iii), we obtain that for any $x \in C^*$ and any standard x_o such that $x_o \simeq x$ must $x_o \in C^*$. Thus, C^{*st} is compact.
The following theorem is a nonstandard and modified version of the famous theorem known by Cantor-Bendixson theorem [17, Theorem 4.1], [18]. Our result is built up to only uncountable condition.

Theorem 2.11. A set $A^* \subseteq \mathbb{R}^*$ contains a Cantor set if and only if A^* contains a closed and uncountable set.

Proof: Let A^* include a Cantor set, say as C^*. Then by Theorem 2.2 and Corollary 2.4, we conclude that C^* is closed and uncountable.
Conversely, assume that A^* contains a closed and uncountable set F^*, then by Cantor-Bendixson theorem [17, Theorem 4.1] the set F^* is contain a perfect subset, say as P^*. Then we have the following two cases:

Case 1. If P^* not contains an interval, then int $(P^*) = \phi$. Hence, P^* is a Cantor set, by Definition 1.16.

Case 2. If P^* contains a nonempty interval, say as $I_r = (x-r, x+r), r \in (R^+)^*$, then $I_r \subseteq P^*$. Let C^* be the Cantor set constructed by third middle part removal process of the closed of the closed interval $\left[x-\frac{\varepsilon}{3}, x+\frac{\varepsilon}{3}\right]$, where $0<\varepsilon<r$. Then $C^* \subset \left[x-\frac{\varepsilon}{3}, x+\frac{\varepsilon}{3}\right] \subset I_r \subseteq P^* \subset F^* \subset A^* \subseteq \mathbb{R}^*$.
Hence, we proved that the set A^* is contain a Cantor set C^*.

Corollary 2.12. If the set $A^* \subseteq \mathbb{R}^*$ contains a closed and uncountable subset, then A^* necessarily include an infinitesimal closed subset, which includes a Cantor set.

Proof: By the converse part of Theorem 2.11 the set A^* contains a perfect subset P^*. Assume that int $(P^*) \neq \phi$, for all $x \in$ int (P^*) there exist $B_r(x) \subseteq P^*$ for standard or nonstandard real number r. Consider unlimited real number ω and take ε to be infinitesimal real number such that $\varepsilon = r/\omega$ in case r is standard, or $\varepsilon = 1/r$ in case r is unlimited and $r > \omega$. Let C^* be the Cantor set constructed by third middle part removal process of the closed interval $\left[x-\frac{\varepsilon}{3}, x+\frac{\varepsilon}{3}\right]$.
Then $C^* \subset \left[x-\frac{\varepsilon}{3}, x+\frac{\varepsilon}{3}\right] \subset B_r(x) \subseteq P^* \subset F^* \subset A^* \subseteq \mathbb{R}^*$.
Hence, we prove that the set A^* is contain an infinitesimal closed subset $\left[x-\frac{\varepsilon}{3}, x+\frac{\varepsilon}{3}\right]$, which includes a Cantor set C^*.

3. Technical applications

Though Euclidean geometry proves highly efficacious in delineating elementary objects characterized by idealized shapes, such as cubes, cones, and cylinders, it encounters limitations when applied to the intricate and irregular structures prevalent in the real world. Complex entities, such as particles undergoing Brownian motion in a fluid, the coastlines of islands, the surface area of the human lung, and the diverse morphologies of natural phenomena like trees and clouds, Plasmons, strange attractors of nonlinear dynamical systems to the distribution of galaxies in the universe, and the distribution of the number of links within web pages. Defy accurate description through classical Euclidean geometry, see Fig. 1. Consequently, the study of such intricate structures has given rise to a burgeoning mathematical discipline known as fractal geometry. A phenomenon considered as Mandelbrot explained it is his paper [19].

Fractals, in essence, manifest as perpetually evolving patterns, exhibiting infinite complexity and self-similarity across diverse scales. Their genesis involves the iterative execution of a fundamental process within an incessant feedback loop. Geometrically, fractals occupy an intermediary dimensionality, transcending our conventional spatial frameworks. Crucially, fractals are not confined solely to natural occurrences; they can be deliberately synthesized through human made.

It is indeed accurate that self-similarity in fractal geometry, while theoretically infinite, is practically limited by the resolution and precision achievable in empirical observations and simulations. In our discussion of the Cantor set and other fractal structures, we acknowledge that the degree of self-similarity that can be observed and utilized in real-world applications is finite, often constrained to a few iterations. This limitation arises due to physical and technological constraints in measurement and computation. Regarding the application of fractals in; Classical or Quantum Mechanics, Music, Brownian Motion, Links on the WWW, …etc. We concur that the precision of experimental data is restricted to a finite number of decimal places. This constraint impacts the extent to which fractal analysis can be applied. However, the utility of fractal geometry in these fields lies not in achieving infinite precision but in providing a robust framework for modeling and understanding complex, irregular phenomena that traditional Euclidean geometry cannot adequately describe. The role of nonstandard analysis in these practical models will be take its strong effect by applying Robinson's Lemma (Lemma 1.14) to increasing the iteration from finite n to unlimited index.

The Fractals method has proven to be efficacious in investigating a myriad of challenges across disciplines such as Physics, Mathematics, Engineering,

Fig. 1. Some samples from the nature of fractal geometry.

Finance, and Biology, for more details see [20]. Notably, fractals have been applied to diverse phenomena, such as mentioned before, one of the examples of applying fractals on Cantor set, see Ziemkiewicz and et al. [21]. These entities can be meaningfully analyzed and understood through the lens of fractal geometry. Fractals gives us a quantitative language to describe the myriad of self-similar shapes found in the natural world, extra examples can be found in Micheel [22]. One of the simplest instances of a fractal is the Cantor set, recognized prior to the formulation of the term "fractals" even emerged [23]. The Cantor set, initially conceived purely under mathematical investigation, has now garnered recognition in the realm of mathematical analysis and its practical applications. This is evident in works by Devaney [24], Hutchinsion [25], Schoenfeld and Gruenhage [26], and Maendes [27]. Among various applications, it holds significance in the realm of dynamical systems, as demonstrated, for instance, by the work of Horiguchi and Morita [28]. The subsequent examples present applications models where we contend that the results obtained in our paper, employing nonstandard tools associated with infinitesimal measure, aptly conform to the behavior exhibited by nanoparticles in nanostructures, notably within the last two models.

3.1. Musical melodies notes

First, we need some fundamental musical terminology that is currently prevalent and essential for our exploration, see [29].

1. *Canon.* In the realm of music, a canon refers to a compositional technique rooted in counterpoint. It involves a melody accompanied by either one or more tradition of the played melody after a specified duration.
2. *Dux.* The opening tune, recognized as the leader or dux, takes the forefront in this musical context.
3. *Bourrée.* A bourrée, found as an optional portion in classical dance suites, is a movement crafted by composers such as J.S. Bach, Handel, and Chopin. Interestingly, these compositions weren't necessarily created for dance.
4. *Ostinato.* Ostinato, derived from the Italian word signifying obstinate or persistent, is a musical term denoting a brief musical phrase or rhythm persistently repeated. This pattern may endure throughout an entire piece or be confined to a specific section. The defining characteristic of an ostinato is its persistent repetition within a musical composition.
5. *Pitch.* Musical notes are associated with specific pitches, which represent the highness or lowness of a sound. The pitch of a note is denoted by letters from A to G, and it may be modified by accidentals (sharps or flats). Changes in pitch direction contribute to the overall shape and character of the melody.
6. *Duration.* Each note has a specific duration, indicating the measure of time it is played. Note durations are expressed using symbols such as whole notes, half notes, quarter notes, eighth notes, etc.
7. *Rhythm.* The arrangement of notes in time creates rhythm, influencing the flow and feel of the melody.
8. *Melodic Contour.* The sequence of ascending, descending, or repeating pitches creates the melodic contour.

To comprehend some of the musical concepts, we can explore the well-known song {Frère Jacques,} a French-origin nursery rhyme available at https://www.youtube.com/watch?v=BC6rvbxdywg. When played in a different tonal range, it is referred to as the follower or counterpart. The follower mimics the leader, replicating its rhythms and intervals precisely or undergoing some form of transformation. Below, we present two musical samples for illustration.

Canons and Fugues: Prominent applied examples of fractals act in music are apparent in canons and fugues. Within a canon, in fact, fractals appear as precise duplicates or altered renditions of the initial musical composition. As an example, we analyze the initial bourreé from Johann Sebastian Bach's Cello Suite No. 3. According to Harlan J. Brothers [30], the initial bourreé in Cello Suite No. 3 stands as an illustration of structural resizing concerning phrasing (see Fig. 2 and https://www.youtube.com/watch?v=xR4IElye7eg). These phrasing elements can be conceptually compared with the Cantor set. In the initial 16 bars of the compilation, there are note sequences displaying a distinct relational pattern, following an A-A-B structure In this context, portion B is twice the duration of portion A.

This musical arrangement, the inherent structured layering within the AAB sequence (short, short, long) is effectively portrayed through the application of a Cantor set map. Each A section, following the AAB pattern, is intricately structured. Illustrated in Fig. 3 is a function detailing the initial 16 point-measures of the composition. The red sections symbolize 4 beats (2 measures) each, the blue sections signify one beat, and the yellow sections represent 1/4 beats (8-th notes). White sections encompass all elements beyond the scope of a

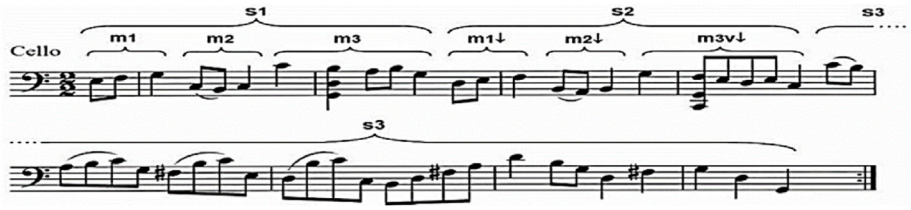

Fig. 2. The initial 16 measures of the first bourrée in Cello Suite No. 3.

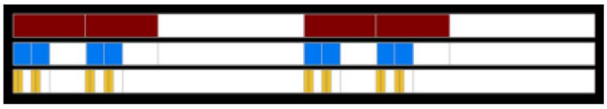

Fig. 3. The Cantor set mapping of the opening 16 point-measures distinctly reveals the nested structure within the phrasing.

concise phrase at each measurement scale. This visualization not just clarifies the fundamental framework of the piece but also reveals the comparative occurrence of its essential components. It especially becomes apparent that, over various stages, when the concise portion extends by a multiple of 4, its occurrence diminishes proportionally by half.

Figure 4 provides an exemplification employing a motif consisting of two notes and two rests, chosen to emulate the Cantor set construction. The exploration of nested sequences possessing a fractal dimension greater than one aligns with the musical analogy of the Koch Curve. An adapted variation is formulated, where each note within the original three-note motif is systematically replaced by three notes, each having half the duration of the original. This gives $D_o = \frac{\ln(3)}{\ln(2)} \simeq 1.58$.

Solo Piano Pó: "Pó" (2008), a solo piano composition named after the Portuguese word for dust,

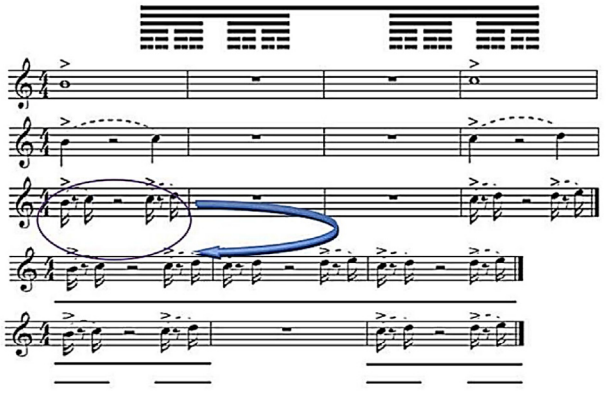

Fig. 4. The Cantor set map of the expected step of plying repeated melody in a smaller duration with similar note in a fast rhythm, for example see https://www.youtube.com/watch?v=Ve3k0WfkFRA.

two-dimensional Cantor set and we denoted it by 2D-Cantor set, stands as another instance of a musical work explicitly grounded in mathematical processes. The conceptual framework of "Pó" is derived from the geometric structure recognized as the Cantor set (see Fig. 5).

With greater precision, "Pó" is structured in accordance with the Cantor set ternary, a geometric arrangement formed through the systematic elimination of the middle thirds within a series of line portions. This process is reiterated until the portions reach a diminutive scale (infinitesimal) akin to that of 2D-Cantor set particles, providing a substantive rationale for the nomenclature of the composition.

In "Pó", the spatial configuration of the Cantor set is communicated through a succession of musical events. This sequential presentation enables the listener, relying on their musical memory, to envision the gradual unfolding of the Cantor set's visual representation. Simultaneously, both complete and incomplete renditions of the set's spatial structure are evident within the musical score. Through repeated exposure and a discerning musical memory, listeners who have observed the score may eventually transfer their visual impressions of the Cantor set into auditory references as well. Given that the piano operates predominantly within the chromatic space concerning pitch, the foundational materials for "Pó" were derived from the twelve notes constituting the chromatic scale. Notably, the number 12 possesses the property of being a multiple of two, three, four, and six, rendering it conducive to the systematic construction of various layers within the Cantor set. Consequently, the initial organization of pitch materials involved the establishment of a twelve-tone row, with its diverse forms serving as line portions of varying sizes. The Cantor set, in turn, influenced the selection of the fundamental cell that served as the origin for the entire row. The conceptual approach involved generating a twelve-note row derived from a tetrachord, as a pitch-class set of this magnitude can equally divide a row into three portions, which is a fundamental principle in constructing a Cantor set. A distinct gesture, depicted in Fig. 6, serves as a

Fig. 5. Similarity of mathematical 2D-Cantor set and musical melody structure.

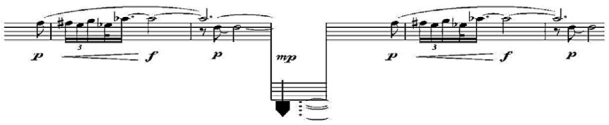

Fig. 6. Lowest cluster of the piano.

spatial metaphor for the Cantor set, comprising three portions. The first and third portions are identical, while the middle one is substituted by the lowest cluster of the piano, it can be of infinitesimal duration, in this case middle cluster can be replaced by silence against an ostinato in the background. The pitches in the first and third portions exhibit symmetrical organization around an axis, and their temporal unfolding towards a tritone bears a resemblance to the process of eliminating the middle part of a line. Vertical rows, wherein the middle part is excised, further contribute to this spatial metaphor.

A gesture that offers a refined representation of the Cantor set's geometry is delineated in Fig. 7. Given the extensive nature of the diagram, we will delineate its overarching contour and subsequently amplify a delimited region to meticulously examine its internal pitch structure. Each twelve-tone row is interspersed with a portion of rests, with a duration identical to that of the respective row. These rests symbolize the omitted middle portion of the Cantor set.

The repetitive recurrence of identical rows facilitates the listener in discerning the resemblance among the melodic lines, thereby constructing an auditory representation of the geometric structure of the Cantor set throughout the work's duration. In the final gesture of the composition, depicted in Fig. 8, the initial twelve-tone row gradually diminishes, metaphorically signifying the dissolution of a line into minute particles, akin to 2D-Cantor set. The repeated time of melody in the next steps follows to the reciprocal measure of the area of the Koch snowflake which is $\left(\frac{2S^2\sqrt{3}}{5}\right)^{-1}$ of the area of the original triangle. Expressed in terms of the side measure s of the original triangle.

With repeated listening and a discerning musical memory, listeners who have encountered the musical score can progressively translate visual references to the Cantor set into auditory associations. Consequentially, as each tone row is interspersed with a portion of rests matching the measure of the respective row, symbolizing the omitted middle portion of the Cantor set. This procedure serves as a direct representation of the Cantor set in the spatial domain. The repeated recurrence of identical rows assists the listener in discerning the similarity among the melodic lines, facilitating the construction of an auditory representation of the geometric design of the Cantor set throughout the duration of the work.

3.2. DNA sequence

The coding sequences in DNA are construed as interconnected clusters within a stochastic Cantor-like set, with non-coding portions aligning with the unoccupied regions of the same set. In the conventional mathematical portrayal of a Cantor set, each tier of repetition consists of discrete points (depicted as dark or filled sites) interspersed with vacant

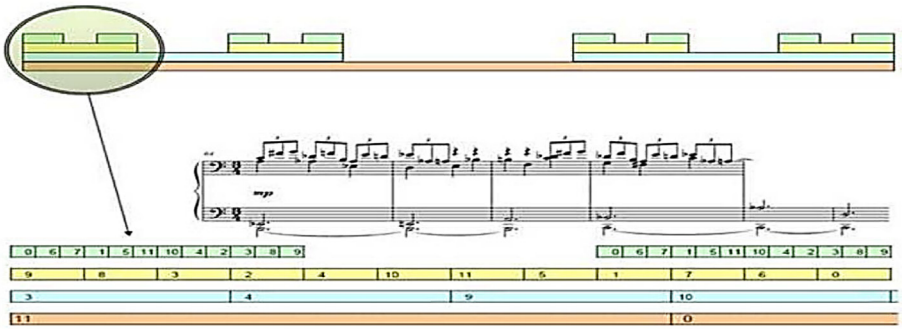

Fig. 7. Zooming of a specific region of musical gesture that represented by Cantor set's to its internal pitch structure.

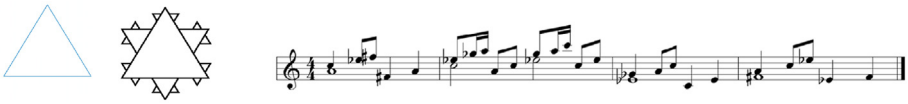

Fig. 8. Last gesture of "Pó" melody similarity to the fractal 2D-Cantor set.

regions, where the quantity of vacant sites proportionally correlates with the system's dimensions [31]. In the suggested explanation, the non-coding sections of DNA are set side by side with the empty areas of a stochastic Cantor set, whereas the coding pieces much up with the inhabited (occupied) locations, see Fig. 9.

All conventional fractals, whether deterministic or random (excluding "fat fractals"), exhibit the following shared characteristics:

- The mass, denoted as $m(s)$ and representing the number of filled sites within the fractal, scales with the size parameter s according to a fractional power law: $m(s) \simeq s^{D_F}$, where D_F denoted to the dimension of the factual.
- The concentration of the fractal decreases to zero when moving towards greater measure scales. This suggests that with an increase in the fractal's measure, the vacant areas eventually encompass almost the entire system, as Takayasu explained in [32, page 127] and [20, page 15].

One can then show that the size distribution of the vacant regions, denoted as $\rho(s)$, adheres to a power law distribution, specifically: $\rho(s) \simeq s^{-D_F-1}$ These structural attributes typical of regular fractals are similarly noticed in DNA chains of more advanced eukaryotes. Specifically, the coding-portions exhibit characteristics aligned with finite measure scales, possessing well-defined average sizes and finite moments, as explicated by Provata and Almirants in their work [33]. Simultaneously, it has been shown that the size distribution of coding portions conforms to distributions at short ranges, as indicated in [17,34].

Conversely, the non-coding portions display moments depending on the system scale, becoming unbounded for systems of unlimited dimensions. The distributions of sizes within these non-coding areas, also referred to as "dividers" due to their function in segregating coding portions, exhibit extended tails and conform to power laws, as demonstrated in [17]. Inspired by the structural similarities between Cantor-like sets and DNA strands, the correlation between them is outlined as below:

DNA		Cantor Set
Coding portions	⇔	Filled Region
Non-coding portions	⇔	Empty Region

Interpretation of DNA sequences with Cantor set

In essence, the regions without coding in a DNA chain are linked with the unoccupied areas within a stochastic Cantor fractal set, whereas the sections with coding correspond to the filled (non-empty) regions The sequences considered in this investigation were selected according to the following conditions: (a) Favoring entire organisms when possible, (b) inclusion of thoroughly documented sequences comprising a significant quantity of coding and non-coding sections, and (c) choosing sequences with the utmost achievable measure.

One of the nonstandard possible criteria for selecting the sequence of DNA chain sequence is its unlimited measure or, biologically speaking, an unbounded size, see Fig. 10. Biologically, it is relatively straightforward to identify sequences meeting such criteria, as a regular fractal predominantly consists of unoccupied regions, and the proportion of occupied regions approaches infinitesimally as the system scale becomes unlimited. In equivalent terms, the noncoding regions (corresponding to

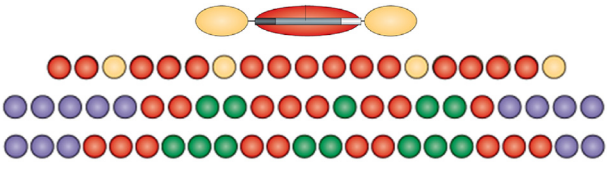

Fig. 9. Random Cantor-like set representation of DNA.

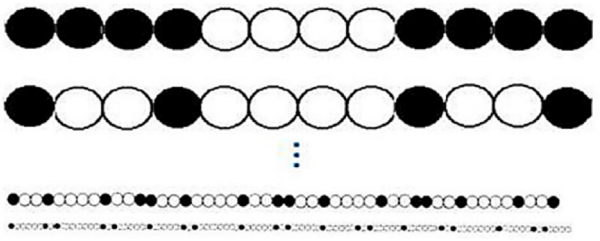

Fig. 10. Nonstandard possible criteria for selecting the sequence of DNA.

unoccupied regions) are expected to encompass nearly the entire genome, while the coding portions should represent an exceedingly infinitesimal percentage of the total genome measure. This unique characteristic is exclusively observed in more advanced eukaryotes.

More than this, the rupture of the DNA sequence is mainly due to protein base mismatch is also has Cantor set structure and properties, Fig. 11.

In various dimensions, the diverse genome sizes of DNA sequences exhibit a state of rupture, as Mandelbrot given it in [19] The analysis of such ruptured DNA sequences involves the application of the Cantor set [33]. According to Theorem 2.7, the Cantor set is both convergent and disconnected. The different measures observed in a DNA sequence converge due to the characteristics of the random Cantor set. The Cantor set remains invariant under homeomorphisms, using this fact and referencing to Fig. 11, a ruptured DNA sequence is conceptualized as a mapping, thereby satisfying the properties of homeomorphisms. According to Theorem 2.7, the DNA sequence is established as non-empty, perfect, and closed. This DNA sequence inherently possesses a Cantor set and exhibits characteristics of a fractal.

Let $N(r)$ be the number of DNA clusters (2D-Cantor remaining subsets) of size r needed to cover all the coding parts of the chain. If D_f is the fractal dimension of the chain, then the number of DNA clusters $N(r)$ scales as $N(r) \simeq r^{-D_f}$.

3.3. Semiconductor materials

Fractal structures have become a focal point of extensive investigation owing to their promising applications in the realm of materials. Notably, the extensively studied cases of smart materials with fractal characteristics encompass self-replicating patterns built upon nanoscale particles. Within this class, self-replicating structures utilizing semiconductor and metallic nanoparticles are particularly intriguing, chiefly because they can be reproduced in laboratory settings.

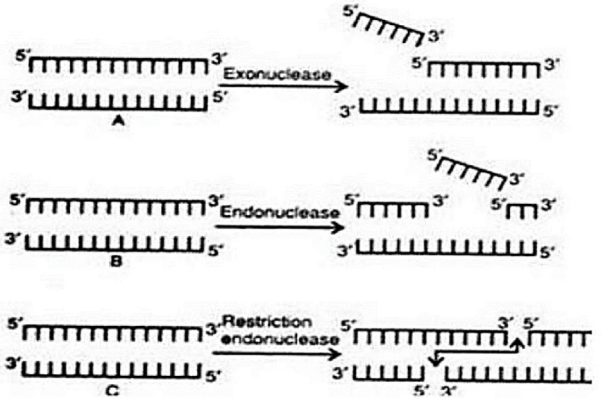

Fig. 11. Ruptured DNA sequence in different genome.

However, existing methods for building structures with similar patterns currently lack precise management or alteration of the specified characteristics. As far as we are aware, electrodynamic trapping remains the exclusive method for crafting a group of nano pieces with a manageable distance between particles and simply geometrically modifiable. An electrodynamic trapping is defined as a setup of electric poles (which physically known as electrode) that produce rapidly oscillating electrical fields.

The organization of electrical potential in traps involves intentionally designed wells for capturing electrically charged particles. Consequently, electrically charged particles are restricted close to the position corresponding to the coordinate of the potential minimum (refer to Fig. 12). Our attention is directed towards electrode geometrical configurations that can characterized as repetition of 2D-Cantor and generalized 2D-Cantor set $(G_n - 2DC)$, chosen for the simplifying their mathematical representation. The fundamental self-quasi-electric pole arrangement with two dimensional portions can be articulated as a 2D-Cantor set.

Symbolizing the i^{th} repetition of 2D-Cantor set, the primary portion (0^{th} -repetition) adopts the shape of a solitary square with sides of measure a. Fig. 13 provides a Three-dimensional visualization of the 2^{nd} repetition of the surface snare, illustrating the electric pole arrangement for the 2^{nd} repetition of 2D-Cantor set. Electric poles are highlighted in pink color, and the first square-area is presented in blue color. The assumption is made that the electric poles are situated in xy - plane, region, while the z - axis is orthogonal to, the electric pole surface, region. In Fig. 13, a green dot signifies the origin of the axes.

At a high index level, the infinitesimal (nano) representation of the electric pole surface will manifest in forms that follow the 2D-Cantor set construction (see Fig. 14).

The global fractal dimension for the generalized Cantor Dust (GnCnD) takes the form $D(p) = \frac{-2\ log\ 2}{log\ ([1\ -\ p]/2}$ where p is the iteratively deleted interval. For the $p = 1/3$ (canonical Cantor Dust), the global fractal dimension is $D(1/3) = 1.26186$, which corresponds to the value $D = \frac{2\ log\ 2}{log\ 3}$

The electrode configurations with the third iteration for $p = 1/5$, $1/10$ and $1/50$ are marked in light blue in Fig. 14(a),(c),(e), respectively. The positions of the potential minima are marked in colored dots in Fig. 14.

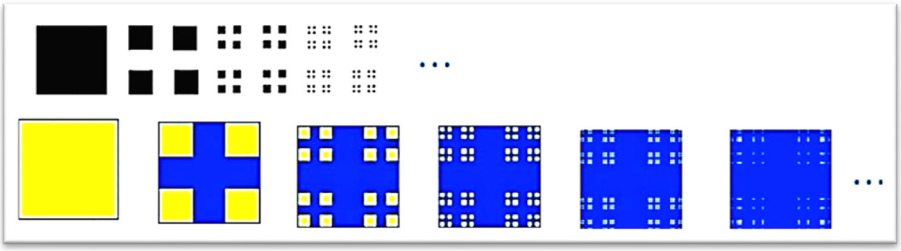

Fig. 12. Cantor set from normal size (first repetition) to infinitesimal (nano) size.

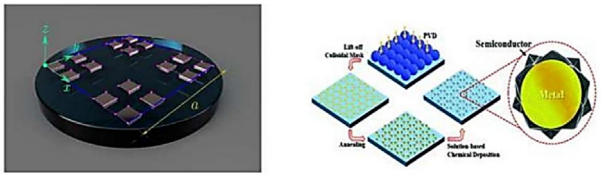

Fig. 13. The surface ion snare showcases a self-quasi-electric pole arrangement for the second repetition of 2D-Cantor set. The measure of the primary portion is labeled as "a", and the electric pole vertices are accentuated in pink.

As demonstrated previously, the electric pole at the 0^{th} repetition is a square, with a side measure of 'a'. The first electric pole arrangement that facilitates stable particle confine is the 1^{st} repetition, comprising four squares, portion (highlighted in blue color in Fig. 14(a)). The positions of minima energy in the xy and xz planes are denoted by green dots in Fig. 14(a) and (b), respectively. It is observed in Fig. 14(a),(b) that the first repetition of the 2D-Cantor set electric pole configuration features five minima energy, represented by green dots. The ratio of the base-sides of the secondand the first order squares corresponds to the ratio of the electric pole square portion sides of the 2^{nd} and 1^{st} repetitions, which is equal to 1/3 in the given model shown in Fig. 14(c),(d).

The application of 2D-Cantor set structure in nanostructures extends to the realm of silicon dioxide layers. Recent strides in nanotechnology have highlighted the potential of nano-capacitors, utilizing densely packed interfaces and thin films [21], to underpin the next generation of energy systems. A method to realize such devices involves constructing multilayer structures with a large (maybe unlimited) surface area within the unoccupied space within a nano structured template, employing atomic layer deposition techniques. Goldhaber-Gordon and et al. in their paper [35] showed that this method holds the potential for scalability, enabling the development of efficient energy stocking systems distinguished by both elevated energy density and high-powered density.

Mathematically, the self-similar behavior implied by the 2D-Cantor set structure should maintain consistency across all scales. However, in the actual world, there exist inherent limits, both upper and lower, beyond which such self-similar behavior is applicable. Although, with using nonstandard analysis technique, one can expected the unlimited repetition of a nano-capacitor characterized by silicon dioxide layers deposited alternately, characterized by their widths that following a 2D-Cantor set arrangement. As an example, the following

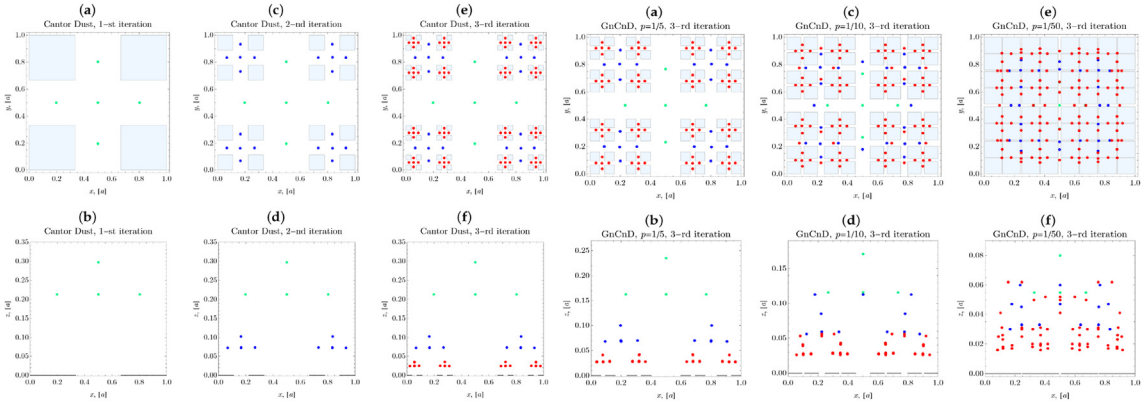

Fig. 14. The positional values of the minima energy in the surface snare featuring 2D-Cantor set electric poles.

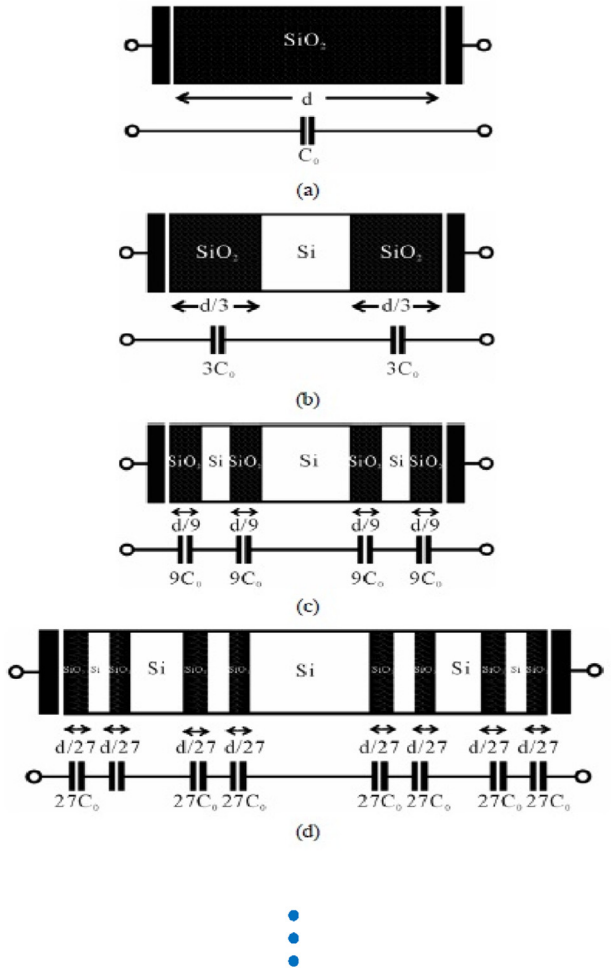

Fig. 15. Nano-capacitor and traditional circuit for the (a) 2D-Cantor set zero repetition generation; (b) 2D-Cantor set first repetition generation; (c) 2D-Cantor set second repetition generation; (d) 2D-Cantor set third repetition generation; ….

Figure represents the conducted utilizing of the self-consistent Schrödinger-Poisson equations for nano-capacitor and traditional circuit, which shows the 2D-Cantor set representation in its structures, as depicted in Fig. 15.

To describe quantum capacitance using a comparable traditional circuit, it is crucial to conceive of a hybrid quantum-traditional model organized in a series-parallel arrangement (see Fig. 16). Nano-capacitor with a 2D-Cantor set multilayered structure formed of silicon dioxide layers presents a traditional and quantum behavior depending on the 2D-Cantor set generation.

The Cantor fractal structure sets a special model for the total capacitance since the distance of the insulator decreases $\frac{d}{3}$ for each generation. The total capacitance per unit area for the zeroth Cantor generation is given by $C_o = \varepsilon_r \frac{\varepsilon_o}{d}$, with d is the distance of insulator decreases and $\varepsilon_r = 3.9$ and C_{Qi} is the quantum capacitance value of i Cantor set generation.

4. Conclusions

This paper presents a novel perspective on the Cantor set through the lens of nonstandard analysis, employing infinitesimal measures to explore its intricate properties. By extending the classical understanding of the Cantor set, we demonstrate how its fractal nature, characterized by self-similarity, can be rigorously quantified using nonstandard tools. Our approach not only provides deeper insights into the measure and dimensionality of the Cantor set but also broadens the scope of fractal geometry in modeling complex structures. The application of infinitesimal measures opens new avenues for analyzing phenomena that exhibit fractal characteristics, thus enhancing our comprehension of both mathematical abstractions and real-world systems.

5. Recommendations

5.1. Further exploration of nonstandard analysis

Researchers are encouraged to delve deeper into nonstandard analysis and its applications to other

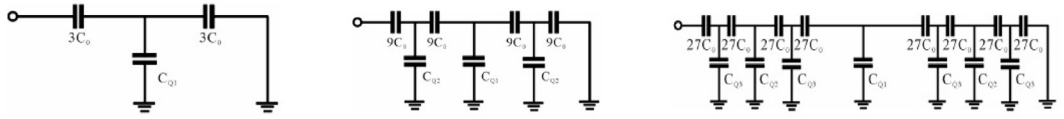

(a) Hybrid traditional quantum circuit model for the first 2D-Cantor set generation.

(b) Hybrid traditional quantum circuit model for the second 2D-Cantor set. generation.

(c) Hybrid traditional quantum circuit model for nanocapacitor device with a Cantor multilayer structure.

Fig. 16. (a) Hybrid traditional quantum circuit model for the first 2D-Cantor set nanocapacitor device generation. (b) Hybrid traditional quantum circuit model for the second 2D-Cantor set generation. (c) Hybrid traditional quantum circuit model for nanocapacitor device with a Cantor multilayer structure.

fractal structures. This approach may uncover new insights and mathematical properties that are not easily accessible through standard methods.

5.2. Experimental validation

We recommend conducting empirical studies to validate the theoretical findings presented in this paper. Applying infinitesimal measures to real-world phenomena, such as nanoparticle behavior in nanostructures, can provide practical evidence supporting the utility of our approach.

Ethics information

This study did not require ethics approval as it did not involve human or animal subjects.

Funding information

The authors state no funding is involved.

Author contributions

All authors contributed with the same percentage in all the sections; drafting, writing, improving, introduce results. All authors have read and agreed to the published version of the manuscript.

Conflict of interest

There were no disclosed conflicts of interest about the research or writing of this work.

References

[1] Nelson E. Internal set theory: a new approach to nonstandard analysis. Bull Am Math Soc 1977;83(6):1165–98. URL: https://www.ams.org/journals/bull/1977-83-06/home.html. https://doi.org/10.1090/s0002-9904-1977-14398-x.
[2] Robinson A. Non-standard analysis. third ed. Princeton, New Jersey: Princeton University Press; 1996. https://doi.org/10.1515/9781400884223.
[3] Tiwari D, Giordano P. Hyperseries in the non-Archimedean ring of Colombeau generalized numbers. Monatsh Math 2022;197:193–223. https://doi.org/10.1007/s00605-021-01647-0.
[4] Goldblatt R. Lectures on the hyperreals: an introduction to nonstandard analysis (Vol. 188). Springer Science & Business Media; 2012.
[5] Qadir C, Aziz W, Hamad I. Rank two integral aspects of three dimensional lotka–volterra equations with nonstandard analysis. Differ Equat Dyn Sys 2023:1–27. https://doi.org/10.1007/s12591-023-00664-9.
[6] Hamad IO, Ismail TH. Generalized curvature and torsion in Nonstandard analysis: nonstandard technical treatment for some differential geometry concepts. Lap Lambert Academic Publishing; 2011.
[7] Keisler HJ. Foundations of infinitesimal calculus (Vol. 20). Boston: Prindle, Weber & Schmidt; 1976. https://people.math.wisc.edu/.
[8] Cutland NJ. Nonstandard real analysis. In: Nonstandard analysis: theory and applications. Dordrecht: Springer Netherlands; 1997. p. 51–76. https://doi.org/10.1007/978-94-011-5544-1_2.
[9] Goldbring I. Lecture notes on nonstandard analysis ucla summer school in logic. URL: https://www.math.uci.edu/; 2014.
[10] Sergio S, Todovov T. Nonstandard analysis in point-set topology Lecture Notes. Vienna: Schrodinger Institute for Mathematical Physics; 1989.
[11] Cohn DL. Measure theory (vol. 5). New York: Birkhäuser; 2013.
[12] Bergman I. Baire category theorem. Mathematics. Master thesis. Karlstads Universiteit 651 88 Karlstad; 2009.
[13] Narayan S. In: Chand S, editor. Elements of real analysis. New Delhi, India: Company Ltd., Ram Nagar; 2009.
[14] Robert A. Nonstandard analysis. John Wiley & Sons Lid; 1988.
[15] Álvarez-Samaniego B, Álvarez-Samaniego W, Ortiz-Castro J. Some existence results on Cantor sets. J Egypt Math Soc 2017;25(3):326–30. https://doi.org/10.1016/j.joems.2017.02.002.
[16] Pawłowicz M. Linear combinations of the classic cantor set. Tatra Mt Math Publ 2013;56(1):47–60. https://doi.org/10.2478/tmmp-2013-0026. URL: https://sciendo.com/pdf/10.2478/tmmp-2013-0026.
[17] Almirantis Y, Provata A. Long-and short-range correlations in genome organization. J Stat Phys 1999;97(1):233–62. https://doi.org/10.1023/A:1004671119400.
[18] Bendixson I. Quelques theorèmes: De la théorie des ensembles de points Extrait d'une lettre adressée à M. Cantor à Halle. Acta Math 1883;2:415–29. https://doi.org/10.1007/BF02612172.
[19] Mandelbrot BB. The fractal geometry of nature (Vol. 1). New York: WH freeman; 1982. p. 25–74. https://doi.org/10.2307/2686529.
[20] Vicsek T. Fractal growth phenomena. second ed. Singapore: World Scientific; 1992. https://doi.org/10.1142/0511. 1992.
[21] Ziemkiewicz D, Karpiński K, Zielińska-Raczyńska S. Fractal Plasmons on Cantor Set Thin Film. Entropy 2019;21(12):1176. https://doi.org/10.3390/e21121176.
[22] Michael FB. Fractals everywhere. Dover Publications, Inc.; 2012.
[23] Khan SI, Islam S. An exploration of the generalized cantor set 2013;2(7):50–4.
[24] Devaney RL. A first course in chaotic dynamical systems. New York: Addition Wesley Publishing Company INC; 1992. https://doi.org/10.1201/9780429503481.
[25] Hutchinson JE. Fractals and self-similarity. Indiana Univ Math J 1981;30(5):713–47. https://doi.org/10.1512/iumj.1981.30.30055.
[26] Schoenfeld AH, Gruenhage G. An alternative characterization of the cantor set. Proc Am Math Soc 1975;53(1):235–6. https://doi.org/10.1090/s0002-9939-1975-0377836-4.
[27] Mendes P. Sum of Cantor sets: self-similarity and measure. Proc Am Math Soc 1999;127(11):3305–8.
[28] Horiguchi T, Morita T. Devil's staircase in a one-dimensional mapping. Phys Stat Mech Appl 1984;126(3):328–48. https://doi.org/10.1016/0378-4371(84)90205-x.
[29] Thomsett MC. Musical terms, symbols and theory: an illustrated dictionary. McFarland; 2016.
[30] Brothers HJ. Structural scaling in Bach's Cello Suite no. 3. Fractals 2019;15(1):89–95. https://doi.org/10.1142/S0218348X0700337X.
[31] Catania S. Role of DNA sequence in CENP-ACnp1 assembly at fission yeast centromeres. Ph.D. thesis. The University of Edinburgh; 2013. https://api.semanticscholar.org/CorpusID:82885490.
[32] Takayasu H. Fractals in the physical sciences. Manchester University Press; 1990.
[33] Provata A, Almirantis Y. Fractal Cantor patterns in the sequence structure of DNA. Fractals 2000;8(1):15–27. https://doi.org/10.1142/s0218348x00000044.
[34] Stephen TK, Jocelyn EK, Elliott SG. Lewin's genes XII. LLC: Jones and Bartlett Learning; 2018.
[35] Goldhaber-Gordon D, Montemerlo MS, Love JC, Opiteck GJ, Ellenbogen JC. Overview of nanoelectronic devices. Proc IEEE 1997;85(4):521–40. https://doi.org/10.1109/5.573739.